JACS
JOURNAL OF THE AMERICAN CHEMICAL SOCIETY
Article
pubs.acs.org/JACS

Thermal and Structural Characteristics of Oligo(3-hexylthiophene)s $(3HT)_n$, $n = 4-36$

Felix Peter Vinzenz Koch,[†] Martin Heeney,[‡,§] and Paul Smith*[,†,§]

[†]Department of Materials, Eidgenössische Technische Hochschule (ETH) Zürich, Wolfgang-Pauli-Strasse 10, 8093 Zurich, Switzerland

[‡]Department of Chemistry and [§]Centre for Plastic Electronics, Imperial College London, Exhibition Rd, London, SW7 2AZ, United Kingdom

ABSTRACT: This study is concerned with the thermal and structural characteristics of a series of precisely defined, monodisperse, regioregular oligo(3-hexylthiophene)s $(3HT)_n$ of $n = 4-36$. We find that these model compounds can feature two distinctly different solid-state structures, i.e., the more classical polymorph Form I in which the hexyl side-chains are not interdigitated and Form II in which they are. The thermodynamic equilibrium melting temperatures of these phases differ as much as ∼180 °C, with 116 °C for Form II and 298 °C for Form I. Furthermore, polymorph II featured an enthalpy of melting of ∼3 times that of Form I and a rate of crystallization that is ∼1 order of magnitude lower than that of Form I. A crossover of the thermodynamically preferred Form II into the kinetically favored Form I is observed at a number of repeat units of 12. In the regime $10 \leq n \leq 21$ the oligo(3-hexylthiophene)s could readily be reversibly converted from one polymorph to another by appropriate processing treatments. The relevance of these findings for the polymeric form (P3HT) is discussed.

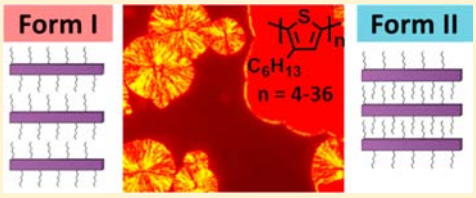

INTRODUCTION

Characteristics of precisely defined oligomers have often provided most relevant insights into related properties of their polymeric counterparts. This is true for, for instance, their equilibrium melting temperatures, which determine the supercooling, ΔT_{sc}, required to induce crystallization for crystallizable species[1,2] and segregation according to their length in polydisperse systems.[3] Further examples are their maximum enthalpy of melting,[2] indicative of secondary molecular interactions as well as their ultimate mechanical[4,5] and electronic properties among other characteristics.

Unlike in the area of mechanics of polymers, many limiting properties of semiconducting macromolecules appear to remain relatively elusive, including but not confined to charge-transport and optimal supra-molecular structure. In view of this fact, we set out to synthesize, as described in an accompanying paper,[6] a homologous series of precisely defined oligomers of the species that is often regarded as one "fruit fly" of organic polymeric semiconductors, i.e., poly(3-hexylthiophene) (P3HT). More specifically, in order to explore certain limits of its characteristics, regioregular oligo(3-hexylthiophene)s $(3HT)_n$ with the number of monomer repeat units of $n = 4-6$, 8−14, 16, 18, 21, 22, and 36 (i.e., a molecular weight range from 667−5988 g/mol) were synthesized. This particular range of low degrees of polymerization was selected as it was established in separate studies that the onset of typical macromolecular issues, such as chain folding, the formation of chain entanglements, etc., although often resulting in beneficial processing and materials properties but hampering generation of accurate data about "limiting" properties, occurs in the regime $n \approx 50-100$[7] (see the excellent review in ref 8 and references therein).

In the present work the focus is on the thermal properties of the above oligomers, which are of obvious relevance for processing and miscibility issues, and structural features, such as polymorphs, that are of potential importance for electronic transport phenomena.

It should be noted, of course, that low molecular weight poly(3-hexylthiophene)s and related oligomers have previously been synthesized.[9−15] However, their polydispersity and/or limited regioregularity leave doubt about the accuracy of their reported properties or, in certain instances, have not been disclosed at all. In addition, the existence of various polymorphs of this class of polymers and its oligomers, both in terms of their molecular arrangement and thermal properties as well as the experimental conditions for their formation are known but apparently have been, and still remain, a matter of confusion and debate,[10,11,15−22] which we aim to resolve in this work employing the precisely defined series of regioregular and monodisperse $(3HT)_n$, $n = 4-36$.

RESULTS AND DISCUSSION

Thermal Analysis. In order to avoid possible influences of synthesis and purification conditions on the properties of the different oligomers, all materials were dissolved in xylene at a concentration of 10 mg/mL, followed by slow evaporation of the solvent during ∼1 h prior to analysis. As the oligomers $(3HT)_n$ with $n \leq 9$ did not yield solids after evaporation of the solvent, the species of $n = 8$ and 9 were stored at room temperature for 24 h. Oligomers of $n = 5$ and 6 were solidified

Received: June 17, 2013
Published: August 19, 2013

   dx.doi.org/10.1021/ja405792b | J. Am. Chem. Soc. 2013, 135, 13699−13709

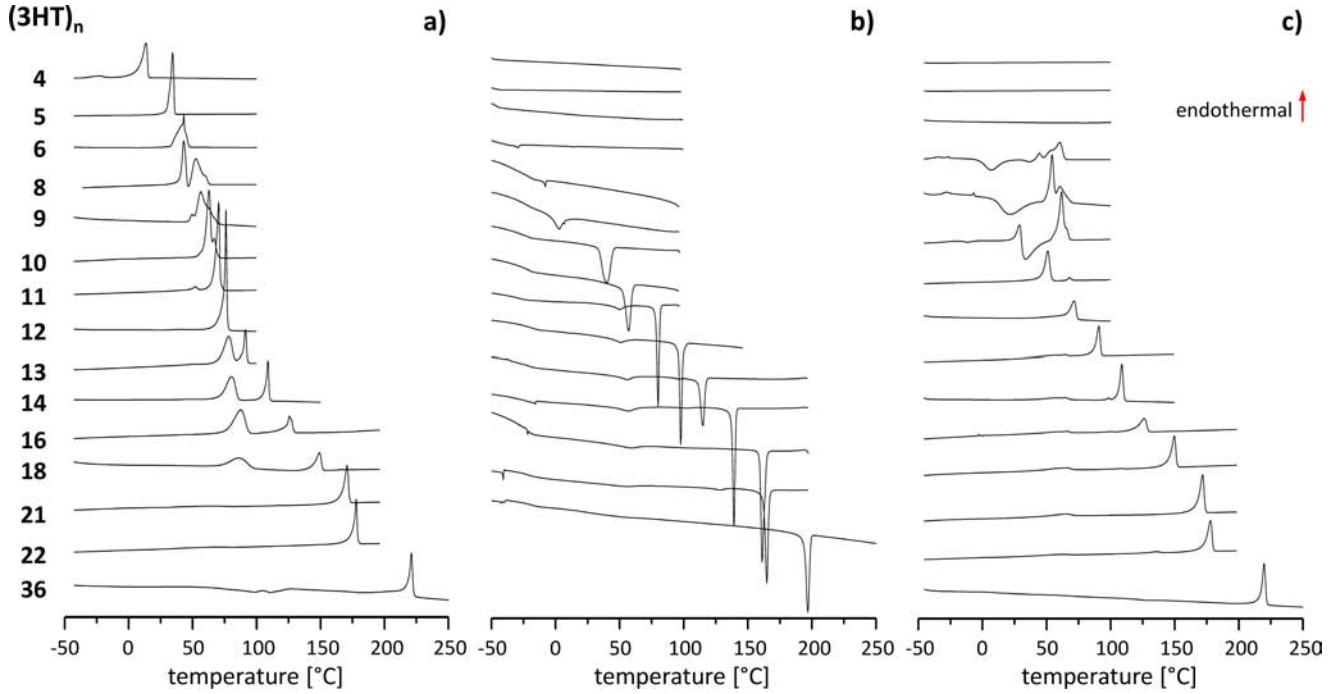

Figure 1. DSC thermograms of $(3HT)_n$ with $n = 4–36$. (a) First heating of crystallized samples (for methods see text); (b) cooling from their melt; and (c) subsequent heating of the material cooled in b). Scan rates 10 °C/min.

at 7 °C for a period of a week, and $(3HT)_4$ was obtained in solid form by storing at −18 °C for 2 weeks.

The samples thus prepared were subsequently analyzed in a first set of experiments at standard heating and cooling rates of 10 °C/min by differential scanning calorimetry (DSC). Figure 1 collects the heating, cooling, and second heating thermograms of the different oligomers. As expected, in general, in the first heating scan their peak melting temperatures, T_m, were found to systematically increase with increasing number of repeat units n. However, $(3HT)_n$ oligomers of $8 \leq n \leq 18$ featured unexpected double or multiple melting endotherms. In the subsequent cooling scan from the melt, the crystallization temperature, T_c, of all oligomers $n \geq 10$ increased with their molecular weight, while for $n \leq 9$ little or no crystallization was observed. Upon second heating of the samples cooled down at 10 °C/min, oligomers of $n \geq 11$ featured only one prominent melting endotherm and those of $n < 8$ only one melting transition in the first heating, no crystallization exotherm and no melting during the second heating scan. Compounds of $8 \leq n \leq 10$ display a rather complex thermal behavior under the conditions applied.

Turning our attention first to oligomers of $n \geq 21$, these compounds featured the expected correlation between the number of repeat units, n, and melting and crystallization transitions, i.e., an increase of T_m and T_c with increasing n. By contrast, the oligothiophenes of $n < 8$, while initially sufficiently crystalline to exhibit a melting endotherm, also at increasing temperatures with increasing value of n, upon cooling at 10 °C/min failed to recrystallize and, hence, did neither display an exotherm nor an endotherm in the cooling and the second heating scans, respectively. Evidently, under these conditions of cooling from the melt, these compounds ($n < 8$) were unable to rearrange into the crystalline order that was obtained by the sample preparation protocol described above. However, when these particular once-molten oligomers were again stored for prolonged periods of time at the low temperatures indicated above (for instance, for 7 days at 7 °C for the compound of n = 5 and 6), they displayed melting transitions similar to those recorded during the first heating cycle, proving that the absence of crystallization during relatively rapid cooling is a kinetic effect and not due to degradation of the material.

The group of $(3HT)_n$ oligomers of $8 \leq n \leq 18$ featured distinct—seemingly nontrivial—thermal characteristics (cf. Figure 1) that will be described and analyzed below. Compounds of: (a) n = 8, 9 exhibited multiple endotherms during the first heating; upon cooling no crystallization occurred; and in the second heating, first a glass transition, followed by an exotherm, and subsequently multiple endotherms were recorded. (b) n = 10 featured a double endotherm during the first heating; upon cooling one broad exotherm; and upon second heating, first a glass transition, followed by an endotherm, an exotherm, and an endotherm. (c) n = 11 exhibited a double endotherm during the first heating; upon cooling one sharp exotherm; the second heating cycle featured one intense endotherm shifted to lower temperature compared to the first followed by the initial endotherm, with a reduced intensity compared to the one recorded for solution-crystallized samples. (d) n = 12 displayed one single endotherm during both the first and second heating scan, the latter shifted by about −5 °C; and a single exotherm during cooling. (e) $13 \leq n \leq 18$ exhibited two endotherms during the first heating; upon cooling one sharp exotherm; and the second heating only showed a pronounced endotherm at the higher temperatures.

In an attempt to unravel the complex thermal behavior observed for the compounds of $8 \leq n \leq 18$, as illustrative examples, oligomers of n = 8, 10, 11, and 13 were subjected in a first set of experiments to a systematic cooling protocol at rates, β, ranging from β = −0.1 to −50 °C/min (see Figure 2 right-hand side), followed by heating at 10 °C/min. In a second set of experiments, the thermal behavior was analyzed of samples prepared by cooling from the melt to −50 °C (β = −10 °C/

dx.doi.org/10.1021/ja405792b | J. Am. Chem. Soc. 2013, 135, 13699−13709

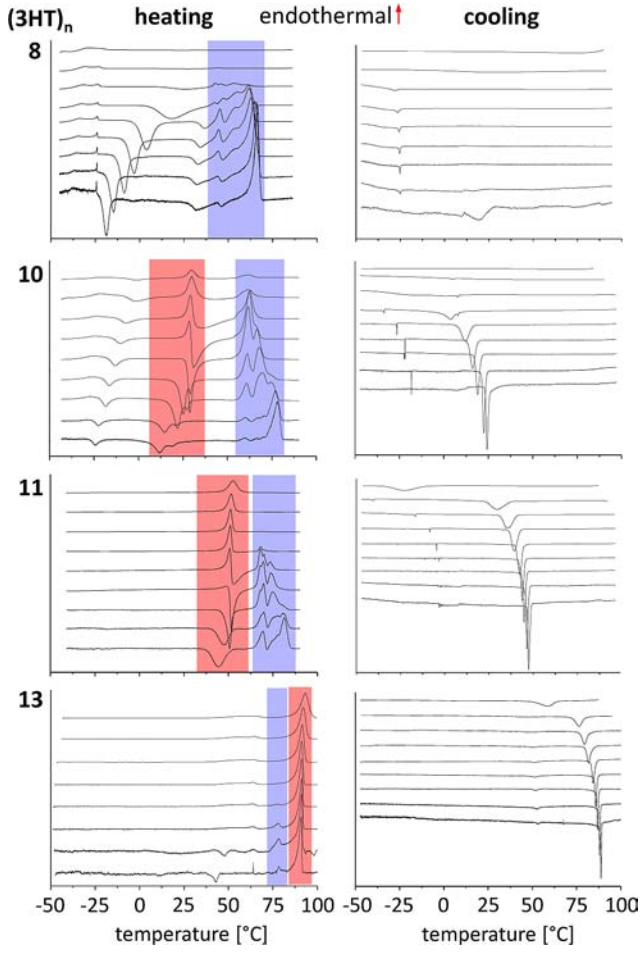

Figure 2. DSC thermograms of oligo(3-hexylthiophene)s n = 8 (first row), n = 10 (second row), n = 11 (third row), and n = 13 (bottom). Left: thermograms recorded at different rates of heating (top to bottom: 50, 20, 10, 5, 2, 1, 0.5, 0.2, 0.1 °C/min) for samples cooled at −10 °C/min from the melt prior to analysis. Right: thermograms recorded at different rates of cooling (top to bottom: −50, −20, −10, −5, −2, −1, −0.5, −0.2, −0.1 °C/min) from the melt.

min) and by heating these at rates β = 0.1 to 50 °C/min. The thermograms of the analysis scans for both sets of experiments are presented in Figure 2.

The results recorded during the heating scan, after cooling at different rates, indicate that $(3HT)_8$ required a large supercooling and a long time for crystallization, while $(3HT)_n$ of n = 10, 11, 13 featured rather sharp recrystallization exotherms already at about 5−20 °C below the endothermic transition marked in red in Figure 2.

The thermograms recorded at various heating rates of samples cooled down from the melt at −10 °C/min to −50 °C, revealed that the initially largely amorphous $(3HT)_8$ only crystallized during heating at rates $\beta \leq 10$ °C/min, with the minimum of the crystallization exotherm shifting to lower temperatures at lower rates (the difference being $\Delta T_c \approx 45$ °C at β = 10 °C/min to β = 0.1 °C/min). The enthalpy of crystallization increased following this trend (ΔH = 8.8 J/g at β = 10 °C/min, while ΔH = 66 J/g at β = 0.1 °C/min). The initially formed crystalline phase subsequently underwent a series of up to four additional apparent melting endotherms with intermittent exotherms, while the temperature of the highest melting transition increased at lower heating rates. These observations suggest a stepwise optimization of the crystalline structure during the heating process possibly due to "healing" an initial mismatch by one or two thiophene repeat units of the oligomers formed in the first instance. (A more detailed description and corroborating indications for this view will be presented in the X-ray Diffraction section.)

The oligomer $(3HT)_{10}$, also largely amorphous when cooled to −50 °C at a rate of $\beta \geq -10$ °C/min, was found to crystallize during heating already at rates of up to β = 50 °C/min at −2 °C and for 0.1 °C/min at −24 °C. This quickly formed crystalline structure melted at about 30 °C and crystallized into an energetically more stable, kinetically slower forming solid. At low heating rates of 2 °C/min and below, endothermal melting was fully dominated by the exothermal crystallization of the new phase of a higher enthalpy of melting. This transformation occurred already below the melting point of the initial phase as a solid−solid transition. The higher melting phase featured similar characteristics as observed for $(3HT)_8$. The thermograms of $(3HT)_{11}$, which already crystallized during cooling, displayed similar features as seen for the decamer but shifted to higher temperatures. The slowly crystallizing, higher melting phase only occurred in detectable quantities at rates of 5 °C/min and below. $(3HT)_{13}$ and higher oligomers crystallized during cooling manifested in a sharp exothermic peak which was hardly affected by the rate of cooling (ΔT_c = 12 °C at β = −20 to −0.1 °C/min). The heating scan of the crystallized samples was essentially unaffected by the cooling rate. It is noteworthy that the additional transition visible in the thermograms of the first heating of solution-cast material (Figure 1) only reoccurred at very low rates of heating ($\beta \leq 1$ °C/min). It appeared as an exothermal solid−solid transition at around 40 °C (at β = 0.1 °C/min), but its melting enthalpy was only a fraction of the value of the solution-cast species. A sample molten once and stored at room temperature for about one month, displayed a small endotherm at the temperature identified as the T_m of the lower melting phase, indeed indicating a solid−solid transition to a thermodynamically more stable form at room temperature.

The kinetic experiments described above strongly suggest that the investigated oligomers on the one hand could feature an extremely fast-forming crystalline polymorph, which was already generated at minimal supercooling (e.g., $\Delta T_c \leq 2$ °C). This solid-state structure will be referred to as the polymorph Form I in the following. On the other hand, these species may slowly form a (thermodynamically more stable) structure, Form II, for which a large supercooling and long time of crystallization are required.

Crystal Growth. In order to obtain insight into differences in mechanism of formation of both phases, isothermal crystallization experiments were conducted and analyzed according to the well-known Avrami equation:[23]

$$\ln(1 - X(t)) = -k_A \cdot t^{n_A} \quad (1a)$$

where $X(t)$ is the degree of crystallinity at time t, k_A a kinetic constant and n_A the Avrami coefficient. For this purpose, the exothermal heat flow during an isothermal crystallization event was analyzed for low degrees of crystallinity (typically below 5%) according to

$$\ln(\Delta H) = n_A \cdot \ln(t) + \ln(-k_A \cdot \Delta H^\circ) \quad (1b)$$

where ΔH° is the enthalpy of melting of a perfect single crystal and ΔH the enthalpy of the (partially) crystallized material. The data thus obtained are presented in Figure 3. Interestingly,

dx.doi.org/10.1021/ja405792b | J. Am. Chem. Soc. 2013, 135, 13699−13709

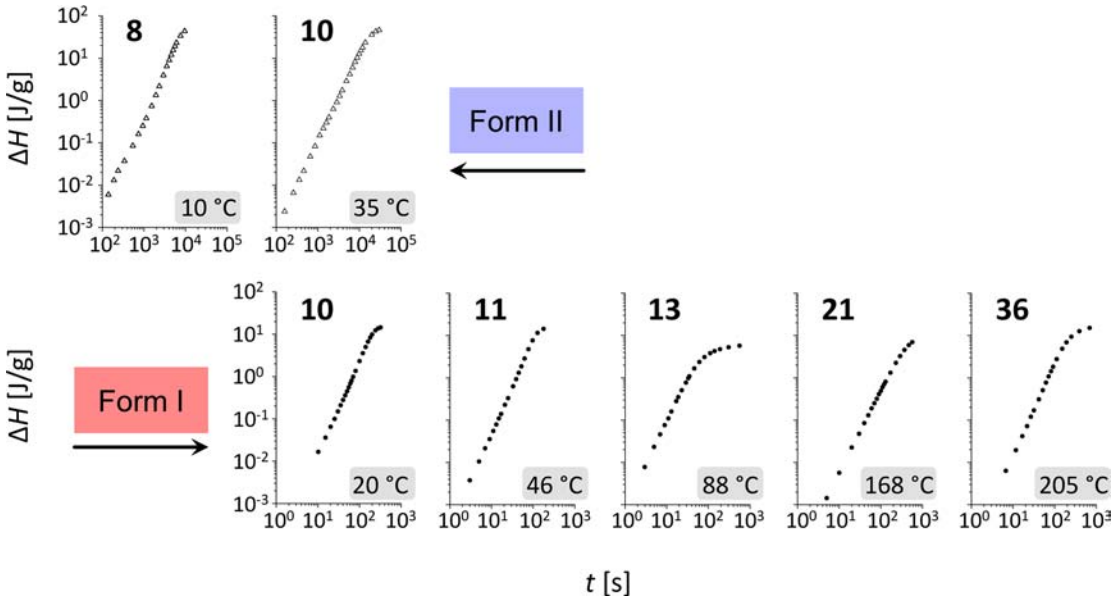

Figure 3. Avrami plots for $(3HT)_n$ (n = 8, 10, 11, 13, 21, 36) in both polymorphs, i.e., slowly crystallizing Form II (top) as well as fast growing Form I (bottom) at the temperatures indicated.

their analysis yielded the conclusion that the Avrami coefficients were found to be essentially independent of the oligomer length and polymorph. Both phases featured a value of $n_A \approx 2$, which is indicative of sporadic nucleation and predominantly one-dimensional crystal growth, which, as a matter of fact, could readily be observed by optical microscopy. Even though crystallization of both polymorphs Forms I and II appeared to be mechanistically similar, their rate of nucleation and crystal growth was found to be vastly different, as already indicated by the thermal analysis results presented in Figures 2 and 3. To further quantify this, the radial growth rates of spherulites and linear crystals generated during isothermal solidification were determined by optical microscopy for the oligomers n = 8 (Form I), 11 (Forms I and II), and 13 (Form II) (Figure 4a), which conveniently featured readily distinguishable "morphologies" (Figure 4b). It was found that the maximum crystal growth rate of Form I was at least 1 order of magnitude higher compared to that of Form II. Unfortunately, the high rate of nucleation of Form I impeded measurements at high supercooling and, therewith, determination of the temperature of maximal crystal growth rate. This was, however, possible for the slowly crystallizing Form II that indeed featured the classical "bell-shaped" growth rate−temperature dependence with maxima at about 25 and 50 °C for $(3HT)_n$ of n = 8 and 11, respectively. While isothermal solidification into Form I occurred already at small supercooling (e.g., ΔT_{sc} = 5 °C for n = 11), almost instantaneously yielding an extremely large number of nuclei allowing fast solidification, in Form II crystallization only commenced at large degrees of supercooling (e.g., ΔT_{sc} = 45 °C for n = 8), even after a long time of settling at this temperature (t > 1 h for n = 8).

Most interesting and revealing, at $T_c \leq 48$ °C $(3HT)_{11}$ crystallized principally in Form I due to the extremely large number of rapidly formed nuclei and at $T_c > 50$ °C solely in Form II, while it crystallized in both polymorphs simultaneously at T_c = 49 °C (see Figure 4b). In other words, the rate of nucleation for both polymorphs was similar at 49 °C, i.e., a supercooling of about $\Delta T_{sc} \approx 1$ °C with respect to the melting point of Form I and as much as $\Delta T_{sc} \approx 30$ °C for Form II.

X-ray Diffraction. The above observations suggest the existence of at least two polymorphs for the $(3HT)_n$, an extremely common feature indeed, and as mentioned above, one that also has already been alluded to in previous reports on poly(3-alkylthiophene)s and related species (cf. ref 8). This assertion was further explored in sets of wide- (WAXD) and small- (SAXD) angle X-ray diffraction studies. Samples were prepared similarly to those for DSC analysis or were crystallized from the melt. Wide-angle X-ray diffractograms of $(3HT)_n$ of n = 5, 8, 10, 11, 16, 18, and 21 are presented in Figure 5.

The oligomers can be grouped according to different characteristic features, as already emerged from the above DSC studies: at a number of repeat units $n \geq 21$, the species predominantly adopted the crystal structure that is commonly observed for their polymeric counterparts of $M_w \gtrsim 10$ kg/mol,[8] typically referred to as type or Form I and already introduced earlier as such, irrespective of the preparation conditions employed here. Compounds of $n \leq 8$, under all of the employed processing conditions, invariably, featured a different molecular order, while in the intermediate regime of $10 \leq n \leq 18$ both polymorphs could coexist, depending on the sample preparation and treatment history. The second polymorph observed featured a (100) signal at q = 5.22 nm^{-1} (about 12 Å). This polymorph was earlier introduced as Form II in accordance with literature.[20,26] It is noteworthy that this rather uncommon structure has rarely been recognized and if, in mixtures with Form I,[20,26] rather than in its pure version as observed here.

In order to further investigate the complex thermal behavior of certain presented oligomers, temperature-dependent wide-angle X-ray analysis was performed in a way that mimics the above-presented DSC experiments. The data obtained are shown here exemplary for $(3HT)_n$, n = 10 (Figure 6) and n = 16 (Figure 7). The samples were prepared as described for the DSC analysis. Initially, both materials were of crystal Form II. The oligomer $(3HT)_{10}$ in Form II, highlighted in blue, melted upon heating at ~75 °C. During cooling from the melt, this

dx.doi.org/10.1021/ja405792b | J. Am. Chem. Soc. 2013, 135, 13699−13709

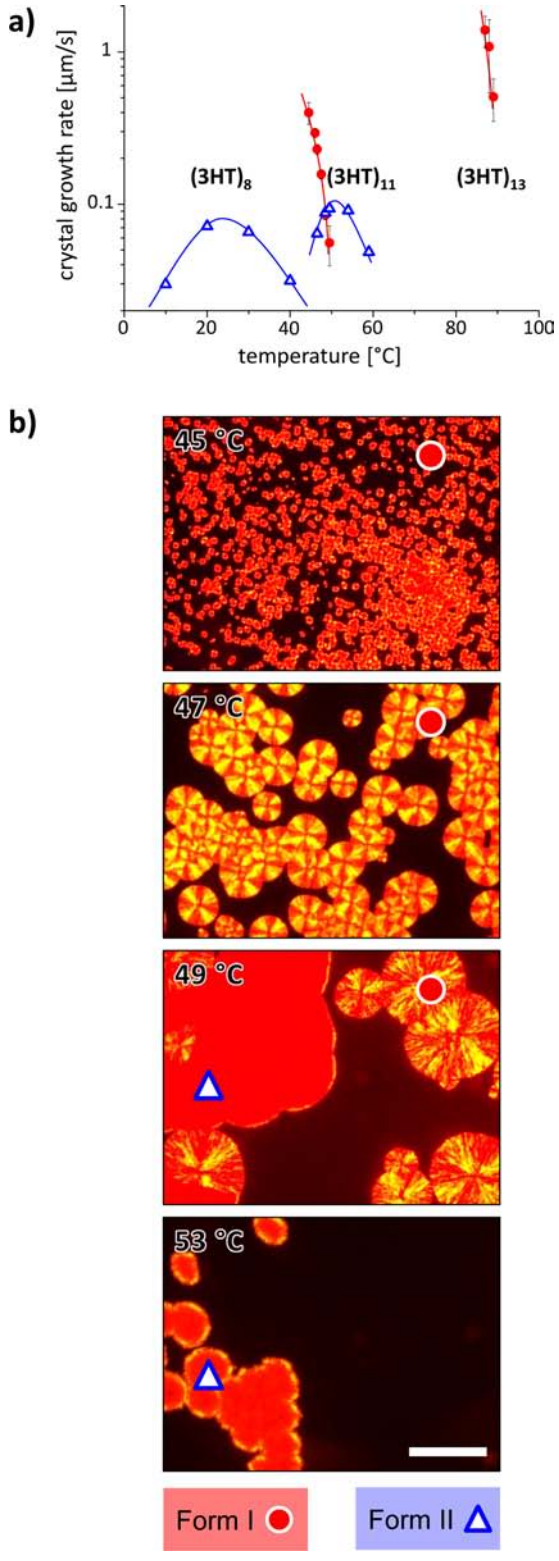

Figure 4. (a) Linear crystal growth rates of oligomers (n = 8, 11, 13) at various crystallization temperatures. Curves are drawn as guidelines to the eye. (b) Optical micrographs of $(3HT)_{11}$ taken during isothermal crystallization at the temperature indicated under crossed polarizers. The scale bar represents 300 μm and applies to all micrographs. Crystals of the polymorphs Form I (filled red circles) and Form II (blue triangles) are indicated in the micrographs by the respective symbols.

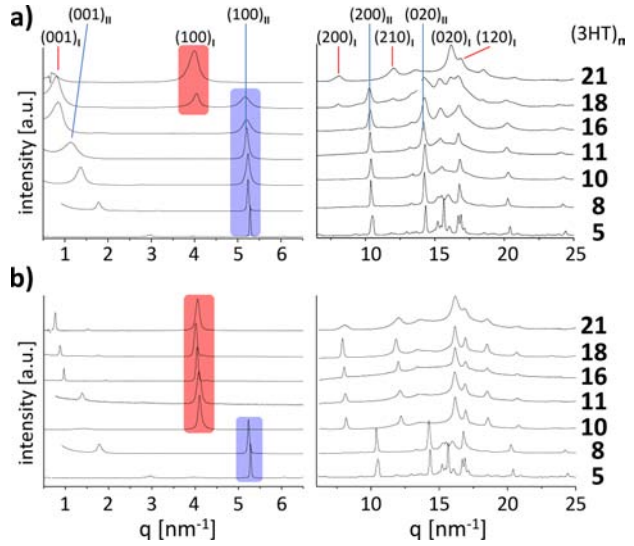

Figure 5. WAXD patterns of $(3HT)_n$, n = 5, 8, 10, 11, 16, 18, and 21: (a) solidified from solution as described for thermal analysis and (b) crystallized from the melt, revealing the polymorphs I (red), II (blue), and mixed phases. The curves in the different graphs are normalized. Indexing of Form I was performed as typically described in literature[15,24] and of Form II assuming analogies to lattices suggested previously for P3ATs.[16,25]

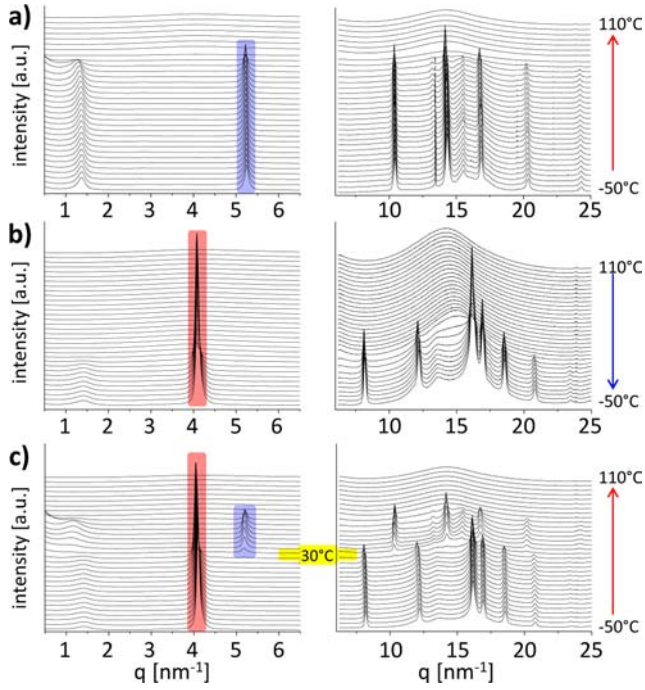

Figure 6. Temperature-dependent wide-angle X-ray diffractograms of $(3HT)_{10}$ recorded at a rate of 10 °C/min illustrating the transition of Form II (blue) to I (red) and vice versa in the temperature range from −50 °C (bottom) to 110 °C (top) in (a) first heating, b) cooling, and c) second heating. Each curve represents a temperature difference of 5 °C.

material crystallized in the polymer-like Form I, highlighted in red, which upon second heating transformed back into Form II at 30 °C (Figure 6a-c).

$(3HT)_{16}$ in the initial Form II (blue) melted during heating at around 85 °C and directly recrystallized in Form I (red), which eventually melted at higher temperatures but upon

dx.doi.org/10.1021/ja405792b | J. Am. Chem. Soc. 2013, 135, 13699−13709

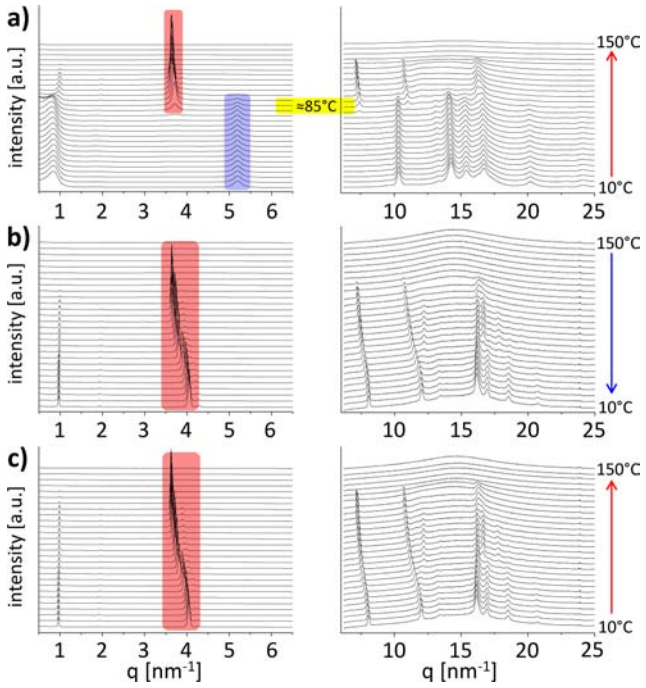

Figure 7. Temperature-dependent wide-angle X-ray diffractograms of $(3HT)_{16}$ recorded at a rate of 10 °C/min reflecting the transition of Form II (blue) to I (red) in the temperature range from 10 (bottom) to 150 °C (top) in (a) first heating, (b) cooling, and c) second heating. Each curve represents a temperature difference of 5 °C.

cooling formed again. During the second heating, in contrast to $(3HT)_{10}$, no thermal transformation into Form II was observed. During cooling as well as second heating, transitions known also for P3HT can be seen. At around 55 °C, as discussed in literature, the side chains melted,[15,21,22] accompanied by an increase in the (100) spacing at higher temperatures. At around 110 °C an additional transition was detected in the X-ray experiments, which was rather faint in DSC (ΔH = 0.5 J/g). During this transition all higher order reflections disappeared except for the (100), (020), and (001) signals, which were still observed above that transition. The structural change involved is most probably a transition into a layered mesophase with smectic symmetry.[15,27] To our knowledge, this transition has been observed only once for a low molecular weight P3HT.[15] Usually unnoticed due to its low intensity, its signal was detected in DSC for oligomers $n \geq 14$ at increasing temperature with increasing molecular weight.

Important information gained from these temperature-dependent wide-angle X-ray experiments is that the relative intensity of the (100) signal being by far the most prominent in Form I is only as intense as the related (020) signal in Form II. The low intensity of the (100) signal in Form II might explain why this polymorph has scarcely been seen or even been overlooked in P3HT.

The presented DSC and X-ray data indicate, indeed, that the oligomer $(3HT)_{10}$ can selectively be crystallized in both phases, which can be converted into one another by simple thermal treatment and annealing processes, e.g., into the faster crystallizing Form I by cooling from the melt (even a rate of 0.1 °C/min is sufficient) and into Form II by annealing the material at a temperature above the melting temperature of Form I (T_m^I = 31 °C) and below that of Form II (T_m^{II} = 70 °C). Similar results were found for the oligomers of n = 11 and 12. The species with $n \geq 13$ were only obtained in Form II, when crystallized from solution by slow evaporation. When crystallized from the melt, the chains got trapped into Form I. For the oligomer n = 21 Form II could be prepared by dissolution in xylene (10 mg/mL) at elevated temperature and storage at 18 °C until precipitation occurred (after about 10 days). The oligomers $n \leq 9$ solidified solely in Form II under the experimental conditions explored in this work.

So far, Form II has principally been observed for low molecular weight P3HT.[20,26] However crystallization from solution of P3HT allowed inducing Form II in P3HT of higher molecular weights. This was shown in cooperation with K. Rahimi (Freiburg, Germany)[28] by transmission electron diffraction, TEM, indicating that Form II is not just a curiosity of low molecular P3HT.

Crystal Structure. Turning now to molecular order, remarkably, definite atomically detailed single crystal structures of the polymorphs Forms I and II have not been resolved, although multitudinous propositions of the unit cell and calculations of possible crystal structures, mostly of Form I, have been reported.[15,24,26,29−39] Hence, in the following we attempt to address some basic structural features, based on SAXD and WAXD, of the present oligo(3-hexylthiophene)s, exploiting their capability to crystallize in both polymorphs. [Note that polymorphism Forms I and II have been reported for other P3ATs (e.g., poly(3-butylthiophene), P3BT,[25,40] poly(3-octylthiophene), P3OT and poly(3-dodecylthiophene), P3DDT)[16] and that for P3BT's Form II a crystal structure has been predicted.[25]]

In Figure 8a−c, the d_{001}-"chain length", d_{100}-"lamellar", and d_{020}-"π-stacking"-related spacings deduced from SAXD and WAXD patterns in Forms I (filled symbols) and II (open symbols) are plotted vs the number of repeat units n. Starting with the d_{001}-"oligomer length"-related spacing in Figure 8a, in addition to the experimental values, the molecular length of each oligomer in its fully extended form, calculated based on the length of one thiophene unit, is also presented. The latter was adapted from literature values of the crystal axis over spanning two thiophene monomers of P3HT (d = 7.8 Å)[8,41] and P3BT (d (Form I) = 7.75 Å,[40] d (Form I) = 7.77 Å[25]). The data unambiguously demonstrate, as expected, that all oligomers solidified into fully extended chain crystals, since in Form I the d_{001} spacings virtually coincide with their molecular length. Interestingly, though, a small but systematical deviation occurred in Form II where the d_{001} spacings were of a somewhat higher value. It seems that in polymorph II the oligomers are not perfectly arranged along their chain axis and that some of them are shifted by one or two thiophene units, which, of course, would cause the crystals to feature a larger d_{001} spacing (see Figure 9).

Turning to the d_{100}-"lamellar" spacing (Figure 8b), this featured an abrupt change from about d_{100} = 12.0 Å in Form II to d_{100} = 15.5 Å in Form I. In the latter polymorph a slight increase of d_{100} with increasing oligomer length was observed from 15.3 Å (n = 10) to 15.8 Å (n = 21), which appears to be consistent with a further increase up to 16.8 Å for high molecular weight P3HT. The width of an oligomer perpendicular to the main axis with straight side chains, considering typical bond angles and lengths, can be calculated to be about 19.8 Å.[42] In Form I these side chains are believed to be arranged at an angle of about 32° with respect to the main chain, which would result in an effective width of 16.8 Å.[42] While in Form I no or negligible side-chain interdigitation is

dx.doi.org/10.1021/ja405792b | J. Am. Chem. Soc. 2013, 135, 13699−13709

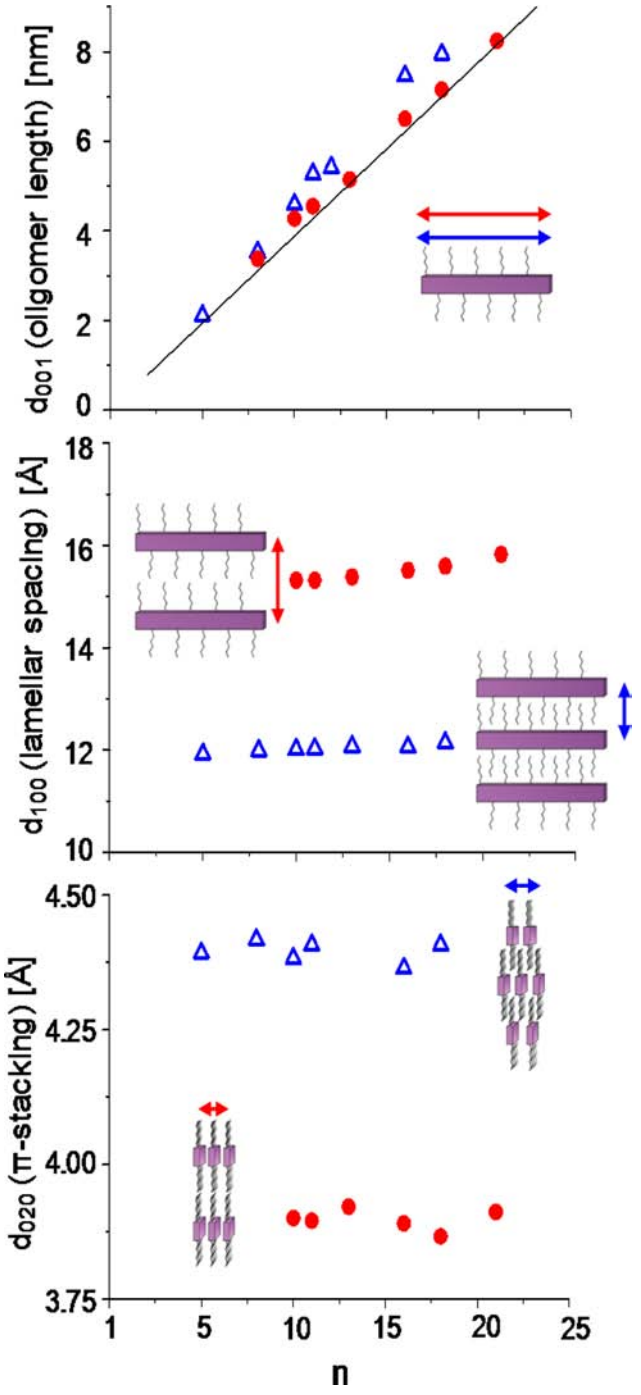

Figure 8. Plots of the d_{001}-oligomer length (a), d_{100}-lamellar spacing, (b) and d_{020}- π-stacking, (c) related spacings vs the number of monomer repeat units n for both polymorphs of $(3HT)_n$ (Form I: red; Form II: blue). The oligomers of $n \leq 8$ possessed the structural features of Form II. For $n > 18$ solely features of Form I were observed, while for the intermediate region $10 \leq n \leq 18$ both polymorphs coexisted.

present, in Form II the rather short d_{100} spacing necessitates such. This is in accordance with a structure model of Form II for P3BT.[25]

In Figure 8c the values of the π-stacking related d_{020}-spacing are plotted vs the number of repeating units. The data related to polymorph Form I of about 3.9 Å are consistent with values reported for P3HT. In Form II the observed d_{020}-spacing was found to be about 4.4 Å, which is a rather long distance for π-stacking in thiophenes.

However, since in this case the π-stacking distance is not coinciding with, but tilted with respect to the d_{020}-distance, (cf. ref 25), the actual π-stacking in this polymorph is shorter than the d_{020} = 4.4 Å.

Revisiting the DSC data for oligomers in Form II, a number of them, e.g., those of n = 8−10, featured multiple endotherms pointing to several different phases, while the temperature-dependent X-ray experiments indicated only "minor changes" in the crystal structure, as major peaks (e.g., (100), (020)) remained at the same position. A conclusion regarding different structures could not be confirmed by X-ray, yet (note though, that for n = 8 and 10 a signal at q = 15.5 nm^{-1} split into two in the range of q = 15.0 −16.0 nm^{-1}). In combination with the d_{001}-spacing being larger than the oligomer itself, as stated above, we suggest that the oligomers in Form II, featuring the interdigitating side chains, do not necessarily always perfectly "zip" into each other during crystallization but are shifted to different extends, i.e., with one or two side chains dangling off (Figure 9). The multiple endotherms in the DSC curves of the different oligomers in this polymorph thus could represent different degrees of perfection of the crystal with respect to d_{001}. This would also be consistent with the fact that solution-crystallized compared to melt-crystallized (β = −10 °C/min) material featured a shorter d_{001}-spacing (Figure 6a,c) and that the enthalpy of melting is higher for the structures having the higher melting point.

Last, but not least, the polymorphism with its structural features discussed above was found to be consistent also with Form II to possess a higher density, ρ, which was determined to be ρ(Form II) = 1.14−1.16 g·cm^{-3} for samples of n = 8 and 11 as well as for solution-cast $(3HT)_{13}$, compared to ρ(Form I) = 1.10 - 1.12 g·cm^{-3} for n = 11, 13, 21 and P3HT, which in turn are consistent with densities calculated from proposed crystal unit cells.[30,35,43]

Finally, it should be noted that a transition from one polymorph into another for oligomers at increasing number of repeat units, n, is rather common. For instance, for oligoethylenes (i.e., normal alkanes or paraffins) of even n, a change from a triclinic to monoclinic molecular packing occurs at n = 26, and subsequently to orthorhombic at n = 28, with the former phase being the more thermodynamically stable for the shorter chains and the latter for those of n > 28—the typical "polyethylene polymorph".[44] Importantly, all structural data presented here for $(3HT)_n$ permit exclusion of any effects that could arise from odd−even monomer repeat unit numbers, as the d-spacings showed no systematically different dependence on them; which is unlike the well-known case of common alkanes.[45]

"Equilibrium" Melting Temperature. A diagram of the melting temperatures (T_m) of the $(3HT)_n$ oligomers, taken as the maximum in heat flow in the DSC thermograms, vs the number of repeat units n is presented in Figure 10 (for the sample preparation see materials and methods). The melting point of Form I of each oligomer in DSC experiments showed no major dependence on its crystallization history. For instance, isothermal crystallization of $(3HT)_{21}$ for 1 h at 170 °C led to a melting temperature of 174.5 °C, while in the DSC at 10 °C/min a melting point of 171 °C was recorded for this oligomer. As discussed above, this relative independence is in strong contrast to materials in the polymorph Form II. For this phase, a shift in melting temperature of up to about 12 °C, depending

dx.doi.org/10.1021/ja405792b | J. Am. Chem. Soc. 2013, 135, 13699−13709

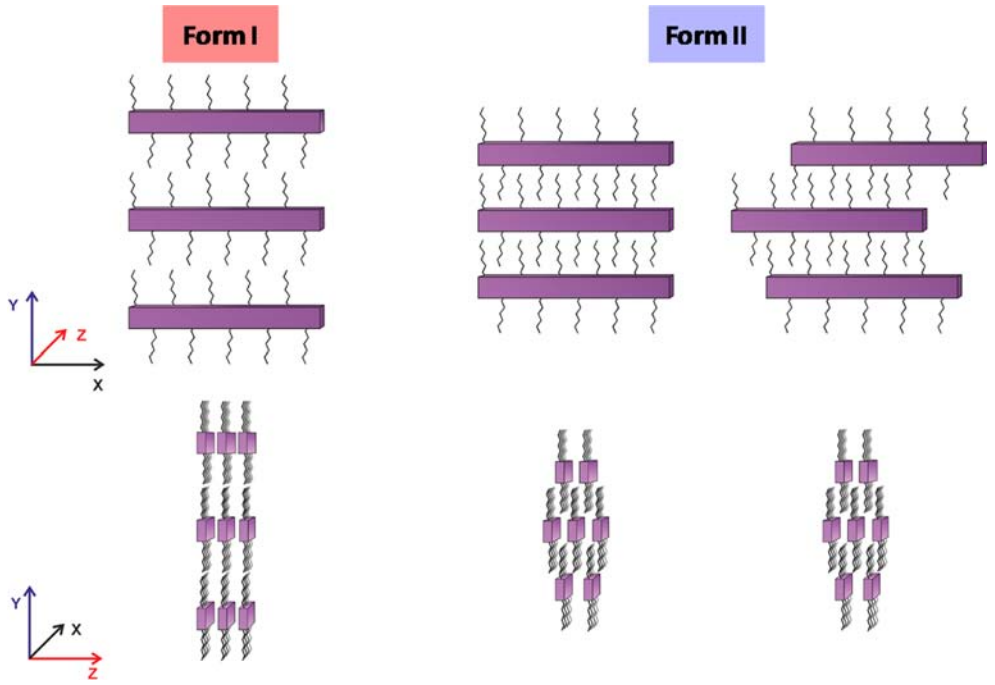

Figure 9. Schematic of the molecular arrangement in the common, polymeric crystalline Form I (left) and Form II. The latter form in its ideal structure (middle) is well arranged along the molecules' main chain, while a certain degree of imperfection due to a shift along the molecules' main chain may occur (right). For oligomers $8 \leq n \leq 12$, the crystals could be transformed into the optimized structure by annealing processes. For simplicity, the side-chain tilt is neglected.

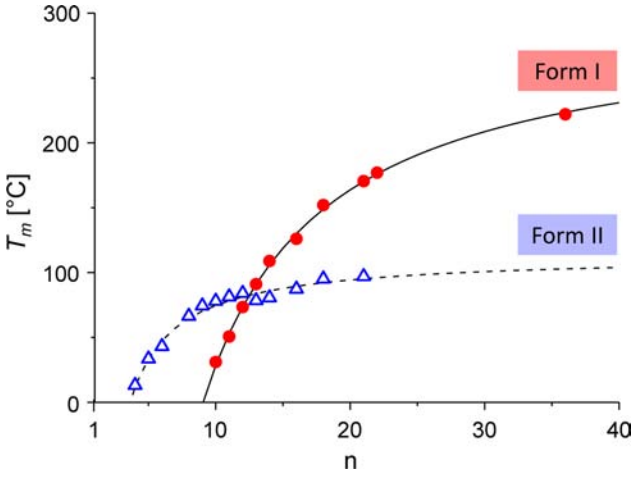

Figure 10. Dependence of the melting temperatures, T_m, of the polymorphs I and II of $(3HT)_n$ on the number of repeat units n. Also plotted are the relations according to Broadhurst,[46] yielding thermodynamic equilibrium values of the two phases of 298 °C (Form I, solid line) and 116 °C (Form II, dashed line), see text.

on the sample's history, was observed. Therefore, the highest measured melting temperature is plotted in Figure 10 for all oligomers, which was typically recorded by slow heating (cf. Figure 2). $(3HT)_{12}$ revealed its highest melting point only after prolonged annealing. Oligomers of $n \geq 13$ could not be prepared in Form II from the melt by thermal treatment and annealing, which impeded the certainty of having perfectly arranged crystals. However, for n up to 21, all materials could be obtained in Form II by dissolution in xylene at a concentration of 10 mg/mL at 80 °C, followed by very slow evaporation of the solvent, typically over 24 h at room temperature or below for $n \leq 18$, while for $n = 21$ storing at room temperature until they precipitated.

The data presented in Figure 10 demonstrate that the oligomers in both polymorphs show the classical increase in T_m with the number of repeat units n.[1,2] Interestingly, $(3HT)_n$ of $n \leq 12$ in Form II featured a higher melting temperature than in Form I, while for those of a larger number of repeat units Form I displayed the higher values of T_m. Also shown in this figure is the dependence of the respective melting temperatures on the number of repeat units n calculated with Broadhurst's well-known equation:[46]

$$T_m = T_m^{\circ}\frac{(n-a)}{(n+b)} \quad (2)$$

Here T_m° is the thermodynamic equilibrium melting temperature (in Kelvin) of infinitely large, defect-free crystals of fully extended, infinitely long chains, and a and b are empirical constants. Employing this relation, thermodynamic equilibrium melting temperatures of 571 and 389 K (298 °C; 116 °C) were derived for polymorph I and II, respectively. The former value is very close to that of 300 °C reported by Malik et al.[47] for the polymeric Form I of P3HT, derived with the Hoffman–Weeks extrapolation.[48] It should be noted, however, that these authors have employed P3HT of finite molecular weight (M_w = 87 kg/mol), whereas the presented extrapolation is directed toward macromolecules of infinite length. For the molecular weight employed by them, this melting temperature according to our calculation should be about $T_{m,\,87k}$ = 291 °C.

Based on melting temperatures of the oligomers n = 4–12, which were annealed to induce the optimized crystal structure, the thermodynamic equilibrium melting temperature of Form II was estimated to be 404 K (131 °C). Reassuringly, this value is in between the melting temperature of Form II reported for P3BT (159 °C)[49] and the temperature at which P3OT

dx.doi.org/10.1021/ja405792b | J. Am. Chem. Soc. 2013, 135, 13699–13709

transformed from Form II into Form I (between 50 and 75 °C).[16]

The enthalpies of melting (ΔH_m) of the oligomers in polymorphs I and II as determined by DSC of optimally solidified samples, i.e., slowly crystallized or long-time annealed just below the highest melting temperature, are presented in Figure 11. From the maximum enthalpy of melting of each

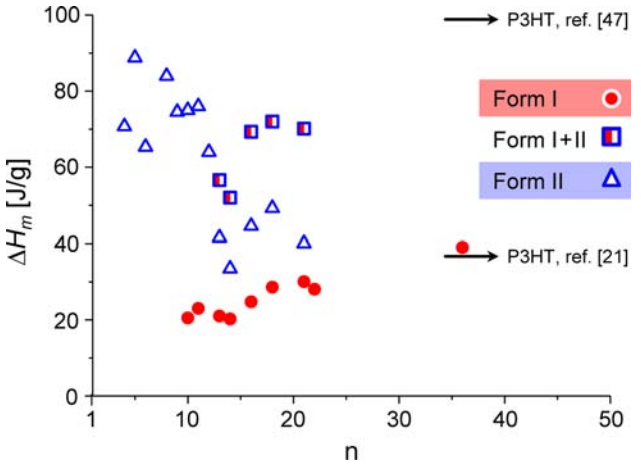

Figure 11. Enthalpy of melting determined by DSC for $(3HT)_n$ in Forms I and II. Oligomers of $n \geq 13$ in Form II immediately recrystallized in Form I during heating. To account for the superposition of endothermic melting and the exothermic crystallization, the sum of ΔH_m° (Form I) and ΔH_m° (Form II) is plotted as well. Literature values of ΔH_m° reported for P3HT are indicated by arrows.[21,47]

phase, we estimated the enthalpy of melting of 100% crystalline material ΔH_m° (Form I) to be about 39 J/g, which is in excellent agreement with the value reported by Pascui et al. for P3HT (ΔH_m° = 37 J/g), who employed solid-state NMR to calculate degrees of crystallinity.[21] Considerably higher values up to ≈90 J/g were estimated for ΔH_m° (Form II). Note for oligomers $n > 12$ the enthalpy of melting of Form II is underestimated when taken from DSC, since during melting of Form II, the melt immediately recrystallizes in Form I. The crystallization enthalpy of this process is masking a significant fraction of the enthalpy of melting of Form II, which is taken into account for in the enthalpy of melting Form I + II. This corrected enthalpy is leveling at around 70 J/g. The reduction in enthalpy of melting of Form II with oligomer length from about 90 to 70 J/g is due to the increasing difficulties to crystallize the material in this polymorph in the perfect structure under the used processing conditions. The higher melting temperature of Form I prohibits annealing of the samples into the perfect structure of Form II.

Interestingly our estimated value for ΔH_m° (Form II) is close to that estimated for P3HT (M_w = 87 kg/mol) crystallized from acetophenone solutions (ΔH_m° = 98 J/g) reported by Malik et al.[47] However we do not believe that Malik and Nandi were able to crystallize P3HT in Form II under the conditions reported, since they crystallize the material at a temperature above our predicted equilibrium melting temperature for Form II of about 116 °C. Rather we believe that the proximity of the values to be coincidental, and a result of the overestimation of crystallinity by a factor of 3 as already described by Pascui et al.[21]

The large difference in values of ΔH_m° (Form I) and ΔH_m° (Form II) appears to be consistent with the suggested difference in molecular packing in the two polymorphs, as schematically presented in Figure 9. In the crystallographic Form II the hexyl side chains are thought to interdigitate, while in the more common Form I they are not; hence in the latter arrangement these moieties are deprived of multiple van der Waals interactions between them.

At first glance it may appear somewhat puzzling that Form II exhibits the higher enthalpy of melting ΔH_m° but is the phase melting at lower temperatures for $n \geq 12$. This, however, is readily understood when considering the entropy of melting ΔS_m° accompanying the melting process, which is calculated according to

$$\Delta S_m^\circ = \Delta H_m^\circ / T_m \quad (3)$$

The compact arrangement of the hexyl side chains due to interdigitation in Form II involves a high degree of order and, therewith, a lower entropy of the solid, compared to the loosely packed alkyl groups in Form I, leading to a considerably higher solid-state entropy. Quantified, for instance, for $(3HT)_{11}$ with eq 3, ΔS_m° ($(3HT)_{11}$, Form II) = 0.214 $J \cdot K^{-1} \cdot g^{-1}$ is no less than three times higher than ΔS_m° ($(3HT)_{11}$, Form I) = 0.071 $J \cdot K^{-1} \cdot g^{-1}$. These differences in values of the entropies of melting were also reflected by the mechanical coherence of the respective materials: somewhat brittle in Form II, while plastic crystalline behavior was observed for Form I. Interestingly Form II is the higher melting phase for oligomers $n \leq 12$. We attribute this to the increasingly adverse contribution of the end groups of the ever shorter oligomers overriding the above entropic considerations. Naturally the side-chain packing would dampen those effects more efficiently in Form II than I.

The thermal properties discussed above are quantitatively summarized in Table 1. The melting and crystallization temperatures of the presented $(3HT)_n$, as well as the enthalpy of melting ΔH_m determined for, e.g., the oligomers n = 21 and

Table 1. Thermal Properties of $(3HT)_n$ of n = 4–36, Their Melting Temperatures under Optimized Conditions T_m^{max}, and Their Highest Enthalpy of Melting Measured in the Two Polymorphs, Forms I and II

$(3HT)_n$, n	$M_n = M_W$ [g/mol]	T_m^{max} (Form I) [°C]	T_m^{max} (Form II) [°C]	ΔH_m^{max} (Form I) [J/g]	ΔH_m^{max} (Form II) [J/g]
4	667	–[a]	13		71
5	833	–[a]	34		89
6	1000	–[a]	43		65
8	1332	–[a]	66		84
9	1499	–[a]	74		75
10	1665	31	78	21	75
11	1831	51	81	23	76
12	1997	73	84	22	64
13	2164	91	79	21	57[b]
14	2330	109	81	20	52[b]
16	2663	126	87	25	69[b]
18	2995	152	95	29	72[b]
21	3494	170	97	30	70[b]
22	3660	177		28	
36	5988	222		39	

[a]If Form I exists, its phase formation was seen neither in DSC nor in X-ray measurements in the samples prepared. [b]Corrected for exothermal crystallization of Form I during melting of Form II.

dx.doi.org/10.1021/ja405792b | J. Am. Chem. Soc. 2013, 135, 13699–13709

36 in Form I are by far higher when compared to values for low molecular weight P3HTs in literature.[20] The latter, reported for samples of M_w in the range of 5.5−10.2 kg/mol are typically in the range of T_m = 166−208 °C and ΔH_m = 12−17 J/g,[7,20,50] while we observed values, for instance, for $(3HT)_{21}$ (M = 3.5 kg/mol) of T_m = 171 °C and ΔH_m = 30 J/g and for $(3HT)_{36}$ (M = 6.0 kg/mol) of T_m = 221 °C and ΔH_m = 39 J/g. We attribute these large differences to the major influence of even the slightest deviation of a polydispersity of unity. In the cited studies, PDI ranged from about 1.28−1.6, while that for the presented oligomers here is, of course, 1. As an illustration, a hypothetic oligomer composed of 1 chain of each of the $(3HT)_n$ with n = 4−36, would feature a value of PDI = 1.23, i.e., of the order of those in ref 20. Clearly, such a material would not be able to form a solid of the perfection presented here and, consequently, would be characterized by lower values of its melting temperature and enthalpy of melting.[3,51]

A further concern is, of course, the influence of even minor presence of regio-irregularity in the chain molecules. In a typical synthetic route to P3HT a PDI = 1.0 combined with 100% regioregularity is rarely observed due to miscouplings induced by the most commonly employed Ni(II)-catalysts. Especially significant for their impact on the materials properties is the location of these miscouplings somewhere within the chain rather than at the chain end.[52,53]

CONCLUSIONS

Thermal and structural characteristics are presented for $(3HT)_n$ with numbers of repeat units n ranging from 4 to 36. The results obtained clearly revealed the existence of two crystal polymorphs, and their thermal properties generally followed the laws of common chain molecules, i.e., increasing melting temperatures with increasing length of the oligomers.

Form I, the polymorph typically observed for the higher molecular weight P3HT, featured a rapid rate of solidification due to a high nucleation rate and fast linear crystal growth and, hence, was found to be kinetically favored. Its enthalpy of melting was found to be relatively low—typical for a mesophase—resulting in a rather high extrapolated thermodynamic equilibrium melting temperature of 298 °C.

Form II is characterized by a high order in the solid due to side-chain interdigitation. Not surprisingly, due to the delicate process of ordering the hexyl side chains, this polymorph was found to exhibit drastically lower rates of nucleation and crystal growth, rendering the creation of this form more affected by processing conditions—increasingly so already at values of the number of repeat units of $n \geq 8$. Its enthalpy of melting was determined to be no less than about three times that of Form I, and this polymorph also naturally featured a distinctly higher density. The high order of its solid-state associated with a large entropy of melting resulted in a rather low thermodynamic equilibrium melting temperature of only 116 °C.

The influence of the structure of both polymorphs on optical and electronic properties of the discussed oligomeric species will be detailed elsewhere.

MATERIALS AND METHODS

Materials. All materials were synthesized as described in an accompanying paper.[6] Chloroform and xylene (isomer mixtures) were purchased from Sigma Aldrich (Buchs, Switzerland).

Sample Preparation. Samples of the different $(3HT)_n$ were crystallized from solution (10 mg/mL) in xylene by slow evaporation of the solvent under nitrogen atmosphere. The oligomers $(3HT)_n$ with $n \leq 9$ did not yield solids after evaporation of the solvent; hence, the species of n = 8 and 9 were stored at room temperature for 24 h. Oligomers of n = 5 and 6 were solidified at 7 °C for a period of 1 week, and $(3HT)_4$ was obtained in solid form by storing at −18 °C for 2 weeks. The maximum enthalpy of melting of $(3HT)_5$ was measured on a sample stored at −18 °C for 6 months. For the preparation of $(3HT)_n$, n = 21, 22 in Form II, 10 mg/mL of the respective oligomer was dissolved in xylene at 80 °C and stored in a sealed vial at room temperature until precipitation occurred to finally evaporate the solvent under a flow of nitrogen.

Optical Microscopy. Optical microscopy was carried out using a Leica DMRX polarizing microscope equipped with a Leica DFC 480 Camera (Leica, Heerbrugg, Switzerland) and a Mettler Toledo FP82HT hot stage (Mettler Toledo, Greifensee, Switzerland).

Differential Scanning Calorimetry (DSC). A Mettler DSC 822^e differential scanning calorimeter (Mettler Toledo, Greifensee, Switzerland), calibrated with indium and zinc, was used to determine melting and crystallization temperatures (T_m, T_c) and enthalpies of melting (ΔH_m). Unless stated otherwise, samples of 1−5 mg of the different compounds sealed in aluminum crucibles were heated and cooled under nitrogen at a standard scanning rate of 10 °C/min. Melting temperatures reported here refer to the maxima of the endothermal peaks. Crystallization kinetics were studied by cooling the samples at a fixed rate of −10 °C/min from the melt to −50 °C, then heating at different rates (50, 20, 10, 5, 2, 1, 0.5, 0.2, 0.1 °C/min), and vice versa, i.e., cooling from the melt to −50 °C at rates of −50, −20, −10, −5, −2, −1, −0.5, −0.2, −0.1 °C/min, followed by analyzing the solidified materials at a constant rate of 10 °C/min. The data shown for low rates of heating and cooling were baseline corrected to allow for data comparison.

Avrami coefficients were determined from the heat flow during isothermal crystallization. As the starting point of the analysis (t_0), the intersection of a baseline, determined from the heat flow after full crystallization, and the heat flow before crystallization was used. The time plotted on the x-axis (Figure 3) corresponds to the reduced time $t - t_0$.

X-ray Diffraction. Variable- and room-temperature SAXD and WAXD measurements were carried out on oligomer samples sealed in glass capillaries of 1.5 mm diameter (Hilgenberg, Malsfeld, Germany) placed in a Linkam THMS600 hot stage, using synchrotron radiation (λ = 1.033 Å) at the Dutch-Belgian beamline (DUBBLE) of the European Synchrotron Radiation Facility (ESRF Grenoble, France).[54] Transmission WAXD patterns were recorded with a Pilatus 300K-W Detector accessing wavenumbers q between 0.12−7.6 nm^{-1} and a Pilatus 1 M in the range of 6.2−46 nm^{-1}. The two-dimensional diffraction patterns were radially averaged after correction for background radiation and calibrated with silver behenate and alpha aluminum. Compounds were drop cast from xylene solutions (10 mg/mL) onto plasma cleaned glass slides. Samples of $(3HT)_{16}$ and $(3HT)_{18}$ were prepared from 20 mg/mL solutions in xylene by slow evaporation of the solvent under a nitrogen atmosphere over 48 h. The oligomer $(3HT)_5$ was transferred into the capillary as an oil and crystallized at 7 °C. All other samples were prepared as described above.

Density Analysis. Densities were determined with a density column (American Density Materials, Inc., Staunton, VA) using deionized water and a saturated aqueous sodium chloride solution at 21 °C, which were degassed prior to use. The gradient was prepared according to standard procedures.[55] The sodium chloride solution was pumped slowly at a constant flow rate and mixed into stirred deionized water. The mixture thus produced was continuously pumped at twice the previous flow rate into the bottom of the density gradient column. The gradient was calibrated with glass spheres of precisely known density (American Density Materials, Inc.). Samples were wetted prior to immersion using a highly diluted aqueous solution of dodecylbenzene sulfonic acid.

AUTHOR INFORMATION

Corresponding Author

paul.smith@mat.ethz.ch

Notes

The authors declare no competing financial interest.

ACKNOWLEDGMENTS

The authors would like the express their gratitude to the DUBBLE Beamline at ESRF (Grenoble, France) for beam time and Giuseppe Portale, for assistance. We would also like to thank the crystallography group of Prof. W. Steurer (ETH Zürich, Switzerland) for the opportunity to use their X-ray equipment and Julia Dshemuchadse for constant support. We thank Jonathan Rivnay and Alberto Salleo (Stanford University, Stanford, CA) for their ongoing efforts in solving the crystal structure of both polymorphs. Natalie Stingelin (Imperial College, London) is acknowledged for her stimulating interest in this work.

REFERENCES

(1) Flory, P. J.; Vrij, A. *J. Am. Chem. Soc.* **1963**, *85*, 3548.
(2) Wunderlich, B. *Crystal Melting*; Academic Press: New York, 1980; Vol. 3.
(3) Matheson, R. R., Jr; Smith, P. *Polymer* **1985**, *26*, 288.
(4) Kausch, H.-H. *Polymer Fracture*; Springer: Berlin, 1987; Vol. 2.
(5) Smith, P.; Lemstra, P. J.; Pijpers, J. P. L. *J. Polym. Sci., Part B: Polym. Phys.* **1982**, *20*, 2229.
(6) Koch, F. P. V.; Smith, P.; Heeney, M. *J. Am. Chem. Soc.* **2013**, DOI: 10.1021/ja4057932.
(7) Koch, F. P. V.; Rivnay, J.; Foster, S.; Müller, C.; Downing, J.; Buchaca-Domingo, E.; Westacott, P.; Yu, L.; Yuan, M.; Baklar, M.; Fei, Z.; Luscomb, C.; McLachlan, M.; Heeney, M.; Rumbles, G.; Silva, C.; Salleo, A.; Smith, P.; Stingelin, N. *Prog. Polym. Sci.* **2013**, http://dx.doi.org/10.1016/j.progpolymsci.2013.07.009
(8) Brinkmann, M. *J. Polym. Sci., Part B: Polym. Phys.* **2011**, *49*, 1218.
(9) Kirschbaum, T.; Azumi, R.; Mena-Osteritz, E.; Bäuerle, P. *New J. Chem.* **1999**, *23*, 241.
(10) Kirschbaum, T.; Bäuerle, P. *Synth. Met.* **2001**, *119*, 127.
(11) Kirschbaum, T.; Briehn, C. A.; Bäuerle, P. *J. Chem. Soc., Perkin Trans. 1* **2000**, 1211.
(12) Gondo, S.; Goto, Y.; Era, M. *Mol. Cryst. Liq. Cryst.* **2007**, *470*, 353.
(13) Tanaka, S.; Tamba, S.; Tanaka, D.; Sugie, A.; Mori, A. *J. Am. Chem. Soc.* **2011**, *133*, 16734.
(14) Masuda, N.; Tanba, S.; Sugie, A.; Monguchi, D.; Koumura, N.; Hara, K.; Mori, A. *Org. Lett.* **2009**, *11*, 2297.
(15) Wu, Z.; Petzold, A.; Henze, T.; Thurn-Albrecht, T.; Lohwasser, R. H.; Sommer, M.; Thelakkat, M. *Macromolecules* **2010**, *43*, 4646.
(16) Prosa, T. J.; Winokur, M. J.; McCullough, R. D. *Macromolecules* **1996**, *29*, 3654.
(17) Meille, S. V.; Romita, V.; Caronna, T.; Lovinger, A. J.; Catellani, M.; Belobrzeckaja, L. *Macromolecules* **1997**, *30*, 7898.
(18) Bidan, G.; De Nicola, A.; Enée, V.; Guillerez, S. *Chem. Mater.* **1998**, *10*, 1052.
(19) Krebs, F. C.; Spanggaard, H. *Sol. Energy Mater. Sol. Cells* **2005**, *88*, 363.
(20) Zen, A.; Saphiannikova, M.; Neher, D.; Grenzer, J.; Grigorian, S.; Pietsch, U.; Asawapirom, U.; Janietz, S.; Scherf, U.; Lieberwirth, I.; Wegner, G. *Macromolecules* **2006**, *39*, 2162.
(21) Pascui, O. F.; Lohwasser, R.; Sommer, M.; Thelakkat, M.; Thurn-Albrecht, T.; Saalwächter, K. *Macromolecules* **2010**, *43*, 9401.
(22) Yuan, Y.; Zhang, J.; Sun, J.; Hu, J.; Zhang, T.; Duan, Y. *Macromolecules* **2011**, *44*, 9341.
(23) Avrami, M. *J. Chem. Phys.* **1939**, *7*, 1103.
(24) Colle, R.; Grosso, G.; Ronzani, A.; Zicovich-Wilson, C. M. *Phys. Status Solidi B* **2011**, *248*, 1360.
(25) Buono, A.; Son, N. H.; Raos, G.; Gila, L.; Cominetti, A.; Catellani, M.; Meille, S. V. *Macromolecules* **2010**, *43*, 6772.
(26) Joshi, S.; Grigorian, S.; Pietsch, U.; Pingel, P.; Zen, A.; Neher, D.; Scherf, U. *Macromolecules* **2008**, *41*, 6800.
(27) Hugger, S.; Thomann, R.; Heinzel, T.; Thurn-Albrecht, T. *Colloid Polym. Sci.* **2004**, *282*, 932.
(28) Rahimi, K.; Botiz, I.; Stingelin, N.; Kayunkid, N.; Sommer, M.; Koch, F. P. V.; Nguyen, H.; Coulembier, O.; Dubois, P.; Brinkmann, M.; Reiter, G. *Angew. Chem., Int. Ed.* **2012**, *124*, 11131.
(29) Joshi, S.; Grigorian, S.; Pietsch, U. In *Organic Electronics*; Wöll, C., Ed.; Wiley-VCH Verlag GmbH & Co. KGaA: Weinheim, 2009, pp 189−205.
(30) Prosa, T. J.; Winokur, M. J.; Moulton, J.; Smith, P.; Heeger, A. J. *Macromolecules* **1992**, *25*, 4364.
(31) Łużny, W.; Trznadel, M.; Proń, A. *Synth. Met.* **1996**, *81*, 71.
(32) Mårdalen, J.; Samuelsen, E. J.; Gautun, O. R.; Carlsen, P. H. *Solid State Commun.* **1991**, *80*, 687.
(33) Tashiro, K.; Kobayashi, M.; Morita, S.; Kawai, T.; Yoshino, K. *Synth. Met.* **1995**, *69*, 397.
(34) McCullough, R. D.; Tristram-Nagle, S.; Williams, S. P.; Lowe, R. D.; Jayaraman, M. *J. Am. Chem. Soc.* **1993**, *115*, 4910.
(35) Brinkmann, M.; Rannou, P. *Adv. Funct. Mater.* **2007**, *17*, 101.
(36) Brinkmann, M.; Rannou, P. *Macromolecules* **2009**, *42*, 1125.
(37) Dag, S.; Wang, L.-W. *J. Phys. Chem. B* **2010**, *114*, 5997.
(38) Xie, W.; Sun, Y. Y.; Zhang, S. B.; Northrup, J. E. *Phys. Rev. B* **2011**, *83*, 184117.
(39) Melis, C.; Colombo, L.; Mattoni, A. *J. Phys. Chem. C* **2010**, *115*, 576.
(40) Arosio, P.; Moreno, M.; Famulari, A.; Raos, G.; Catellani, M.; Meille, S. V. *Chem. Mater.* **2008**, *21*, 78.
(41) Kayunkid, N.; Uttiya, S.; Brinkmann, M. *Macromolecules* **2010**, *43*, 4961.
(42) Chen, S. A.; Ni, J. M. *Macromolecules* **1992**, *25*, 6081.
(43) Tashiro, K.; Kobayashi, M.; Kawai, T.; Yoshino, K. *Polymer* **1997**, *38*, 2867.
(44) Craig, S. R.; Hastie, G. P.; Roberts, K. J.; Sherwood, J. N. *J. Mater. Chem.* **1994**, *4*, 977.
(45) Lüth, H.; Nyburg, S. C.; Robinson, P. M.; Scott, H. G. *Mol. Cryst. Liq. Cryst.* **1974**, *27*, 337.
(46) Broadhurst, M. G. *J. Chem. Phys.* **1962**, *36*, 2578.
(47) Malik, S.; Nandi, A. K. *J. Polym. Sci., Part B: Polym. Phys.* **2002**, *40*, 2073.
(48) Hoffman, J. D.; Weeks, J. J. *J. Res. Natl. Bur. Stand., Sect. A* **1962**, *66*, 13.
(49) Lu, G.; Li, L.; Xiaoniu Yang. *Macromolecules* **2008**, *41*, 2062.
(50) Reid, O. G.; Malik, J. A. N.; Latini, G.; Dayal, S.; Kopidakis, N.; Silva, C.; Stingelin, N.; Rumbles, G. *J. Polym. Sci., Part B: Polym. Phys.* **2012**, *50*, 27.
(51) Smith, P.; Manley, R. S. J. *Macromolecules* **1979**, *12*, 483.
(52) Kohn, P.; Huettner, S.; Komber, H.; Senkovskyy, V.; Tkachov, R.; Kiriy, A.; Friend, R. H.; Steiner, U.; Huck, W. T. S.; Sommer, J.-U.; Sommer, M. *J. Am. Chem. Soc.* **2012**, *134*, 4790.
(53) Tkachov, R.; Senkovskyy, V.; Komber, H.; Sommer, J.-U.; Kiriy, A. *J. Am. Chem. Soc.* **2010**, *132*, 7803.
(54) Bras, W. *J. Macromol. Sci., Part B: Phys.* **1998**, *37*, 557.
(55) Wunderlich, B. *Crystal Structure, Morphology, Defects*; Academic Press: New York, 1973; Vol. 1.